British Journal of Pharmacology

British Journal of Pharmacology (2017) **174** 3000–3017 3000

RESEARCH PAPER

# Inhibition of JNK signalling mediates PPARα-dependent protection against intrahepatic cholestasis by fenofibrate

**Correspondence** Aiming Liu, Medical School of Ningbo University, Ningbo 315211, China. E-mail: liuaiming@nbu.edu.cn

**Received** 10 February 2017; **Revised** 1 June 2017; **Accepted** 16 June 2017

Manyun Dai[1,*], Julin Yang[2,*], Minzhu Xie[1], Jiao Lin[1], Min Luo[1], Huiying Hua[1], Gangming Xu[1], Hante Lin[1], Danjun Song[1], Yuqing Cheng[3], Bin Guo[3], Jinshun Zhao[1], Frank J Gonzalez[4] and Aiming Liu[1]

*[1]Medical School of Ningbo University, Ningbo, China, [2]Ningbo College of Health Sciences, Ningbo, China, [3]Hunan Normal University, Changsha, China, and [4]Laboratory of Metabolism, National Cancer Institute, NIH, Bethesda, MD, USA*

*These authors contributed equally to this work.

## BACKGROUND AND PURPOSE

Fenofibrate, a PPARα agonist, is the most widely prescribed drug for treating hyperlipidaemia. Although fibrate drugs are reported to be beneficial for cholestasis, their underlying mechanism has not been determined.

## EXPERIMENTAL APPROACH

Wild-type mice and *Pparα*-null mice were pretreated orally with fenofibrate for 3 days, following which α-naphthylisothiocyanate (ANIT) was administered to induce cholestasis. The PPARα agonist WY14643 and JNK inhibitor SP600125 were used to determine the role of PPARα and the JNK pathway, respectively, in cholestatic liver injury. The same fenofibrate regimen was applied to investigate its beneficial effects on sclerosing cholangitis in a DDC-induced cholestatic model.

## KEY RESULTS

Fenofibrate, 25 mg·kg$^{-1}$ twice a day, totally attenuated ANIT-induced cholestasis and liver injury as indicated by biochemical and histological analyses. This protection occurred in wild-type, but not in *Pparα*-null, mice. Alterations in bile acid synthesis and transport were found to be an adaptive response rather than a direct effect of fenofibrate. WY14643 attenuated ANIT-induced cholestasis and liver injury coincident with inhibition of JNK signalling. Although SP600125 did not affect cholestasis, it inhibited liver injury in the ANIT model when the dose of fenofibrate used was ineffective. Fenofibrate was also revealed to have a beneficial effect in the sclerosing cholangitis model.

## CONCLUSIONS AND IMPLICATIONS

These data suggest that the protective effects of fenofibrate against cholestasis-induced hepatic injury are dependent on PPARα and fenofibrate dose, and are mediated through inhibition of JNK signalling. This mechanism of fenofibrate protection against intrahepatic cholestasis may offer additional therapeutic opportunities for cholestatic liver diseases.

## Abbreviations

ALP, alkaline phosphatase; ALT, alanine aminotransferase; ANIT, α-naphthylisothiocyanate; AST, aspartate aminotransferase; BSEP, bile salt export pump; c-Jun, AP-1 transcription factor subunit; Cyp7a1, cholesterol 7α-hydroxylase; Cyp8b1, sterol 12α-hydroxylase; DBIL, direct bilirubin; DDC, 3,5-diethoxycarbonyl-1,4-dihydrocollidine; FA, fenofibric acid; MDR2, multidrug resistance protein 2; MKK4, mitogen-activated protein kinase kinase 4; MRP3, multidrug resistance-related protein 3; MRP4, multidrug resistance-related protein 4; OATP1, organic anion transporting polypeptide 1; OSTB, organic solute transporter-β; p65, NF-κB p65 subunit; TBA, total bile acid; TBIL, total bilirubin; UDP, uridine diphosphate

DOI:10.1111/bph.13928

## Introduction

**Fenofibrate** is an agonist for the nuclear hormone receptor **PPARα**. Clinically, fibrates are widely used for the treatment of hypertriglyceridaemia and mixed hyperlipidaemia associated with atherosclerosis (Fievet and Staels, 2009). After activation by agonists, PPARα dimerizes with the retinoic X receptor and binds to the peroxisome proliferator response elements upstream of target genes involved in the metabolism and transport of lipids (Peters *et al.*, 2005). Fibrates are also effective for the treatment of metabolic diseases such as diabetes and hypertension, as well as protection against hepatotoxins such as acetaminophen (Day *et al.*, 1993; Patterson *et al.*, 2012; Song *et al.*, 2016).

Cholestasis, including primary biliary cholangitis (PBC) and primary sclerosing cholangitis (PSC), often results in the retention of bile salts (Hirschfield *et al.*, 2010). This occurs when the balance of production and transport of bile acids is disrupted, leading to liver fibrosis, cirrhosis and liver failure. In northern Europe, the incidence of PBC was estimated to be between 1 and 49 cases per million people year$^{-1}$, and the prevalence was between 7 and 402 per million people (Prince and James, 2003; Lazaridis and Talwalkar, 2007; Poupon, 2010). In Asian countries, the prevalence of PBC was 400–500 cases per million (Sakauchi *et al.*, 2005; Liu *et al.*, 2010). For PSC, the published incidence was as high as 1.3/100 000 year$^{-1}$ and the prevalence was 16 per 100 000 people (Lindkvist *et al.*, 2010; Molodecky *et al.*, 2011; Boonstra *et al.*, 2012; Hirschfield *et al.*, 2013). More than 50% of PSC patients need liver transplantation 10–15 years after the development of symptoms (Broome *et al.*, 1996; Tischendorf *et al.*, 2007; Claessen *et al.*, 2009). Ursodeoxycholic acid (UDCA) slows the progression of PBC in stages I and II. Despite the beneficial effects, UDCA remains ineffective in up to 50% of patients (Kaplan and Poupon, 2009; Carbone *et al.*, 2013). In 2016, obeticholic acid was approved by the FDA for the treatment of PBC. Thus, there is still a great need for additional therapeutic options for cholestatic disease.

Besides its involvement in the metabolism of lipids, glucose and amino acids, PPARα has a role in bile acid homeostasis (Zhou *et al.*, 2014). In mice treated with the PPARα agonist **WY14643** for 7 days, expression of the bile acid synthesis enzyme **CYP8B1** (sterol 12α-hydroxylase) increases by fivefold, resulting in altered bile acid homeostasis (Hunt *et al.*, 2000). The PPARα activator gemfibrozil induces an up-regulation of cholesterol 7α-hydroxylase (**CYP7A1**) and CYP8B1 and increases total bile acids (TBAs) in a dose-dependent manner in wild-type mice but not in *Pparα*-null mice (Liu *et al.*, 2014a). In a colitis model, activation of a PPARα–UDP–glucuronosyltransferase signalling pathway accelerated the elimination of intestinal bile acids, resulting in suppression of farnesoid X receptor-FGF15 signalling. The subsequent up-regulation of hepatic CYP7A1 promoted the *de novo* synthesis of bile acid (Zhou *et al.*, 2014). In *Pparα*-null mice administered a cholic acid diet, an elevation of taurocholic acid and cholic acid was observed. In contrast, neither the latter metabolic disorder nor the effect on bile acid synthesis was noted in wild-type mice (Li *et al.*, 2012). These findings suggest that PPARα can have both a protective and a disruptive role in bile acid homeostasis.

Fibrate drugs are used to treat patients with chronic cholestatic liver disease refractory to UDCA monotherapy in the clinic. In 19 patients with early-stage PBC and an inadequate response to UDCA, treatment with UDCA plus bezafibrate for 3 months significantly improved serum biliary enzymes, IgM and cholesterol (Honda *et al.*, 2013). In 20 PBC patients who inadequately responded to UDCA, serum alkaline phosphatase (ALP) decreased from 214–779 to 60–384 U·L$^{-1}$ when fenofibrate was administered in combination with UDCA for 48 weeks, (Levy *et al.*, 2011). In a retrospective cohort study, fenofibrate was associated with a significant improvement in ALP levels in PBC patients with an incomplete response to UDCA (Cheung *et al.*, 2016). In PBC patients treated with fenofibrate plus UDCA and bezafibrate plus UDCA, the serum ALP, γ-glutamyl transpeptidase and serum immunoglobulin M levels in the two groups were substantially improved compared with their baseline levels, indicating a therapeutic effect (Dohmen *et al.*, 2013). Although their therapeutic efficacy is evident, there is still no clinical guidelines directing fibrates for the treatment of cholestasis, and thus, physicians are reluctant to prescribe fenofibrate to cholestatic patients.

In rat hepatocytes, ciprofibrate and WY14643 reduce *Cyp7a1* and *Cyp27a1* mRNA levels along with a reduction in enzymatic activities (Post *et al.*, 2001). In HepG2 cells, fenofibrate up-regulates the expression of human multidrug resistance protein 3 (MDR3, MDR2 in mouse; also known as **ABCC2**). And when incubated with rat isolated hepatocytes, fenofibrate increases the canalicular excretion of phosphatidylcholine (Ghonem *et al.*, 2014). Fibrates and WY14643 reduce p65 (NF-κB p65 subunit)-mediated activation of **IL-1β** by inducing the expression of the inhibitory factor IκBα in a PPARα-dependent manner (Delerive *et al.*, 2000). Thus, several mechanisms for the effects of fenofibrate against cholestasis that involve PPARα have been proposed, including the down-regulation of CYP7A1, up-regulation of MDR3 (ABCC2) and an anti-inflammatory action mediated by inhibiting NF-κB (Ghonem *et al.*, 2015). However, these studies were largely based on *in vitro* models and non-cholestatic models.

In the present study, ANIT (α-naphthylisothiocyanate)-induced cholestasis and liver injury were evoked in a mouse model to evaluate the protective effect of fenofibrate. Wild-type and *Pparα*-null mice were used to determine the role of PPARα. Three doses of fenofibrate (5, 25 and 125 mg·kg$^{-1}$ twice a day), the PPARα agonist WY14643 and **JNK** inhibitor **SP600125** were used to explore the underlying mechanism. The data demonstrated that both PPARα and the dose used were critically important for the anti-cholestatic action of fenofibrate. JNK signalling was found to mediate the cholestatic liver injury and the protective effect of the PPARα agonist was mediated by inhibiting this signalling pathway.

## Methods

### *Animals*

All animal care and experimental procedures conformed to the Animals (Scientific Procedures) Act 1986 of the UK Parliament, Directive 2010/63/EU of the European Parliament and

the Guide for the Care and Use of Laboratory Animals published by the US National Institutes of Health (NIH Publication No. 85–23, revised 1996). Ethical approval was granted by the Animal Welfare and Ethics Review Board of the Medical School of Ningbo University, China. Animal studies were reported in compliance with the ARRIVE guidelines (Kilkenny *et al.*, 2010; McGrath and Lilley, 2015). The effect in a minimum of five mice per group was chosen as calculated by GPOWER.

ANIT-induced cholestasis and liver injury were evoked in a mouse model to evaluate the protective effect of fenofibrate. Wild-type and *Pparα*-null mice were used to determine the role of PPARα. Three doses of fenofibrate (5, 25 and 125 mg·kg$^{-1}$ twice a day), the PPARα agonist WY14643 and JNK inhibitor SP600125 were used to explore its underlying mechanism. Prior to the experiments, male 8 to 10 week (24 to 28 g) wild-type and *Pparα*-null mice on the 129/Sv background were housed at the Medical School of Ningbo University Animal Services Unit (SPF) for 7 days at 23 ± 1°C, with a relative humidity of 60–70% and a light/dark cycle of 12 h with free access to water and standard mouse chow. The mice were kept in standard cages ($n$ = 5) with aspen bedding.

The wild-type mice were divided into eight groups ($n$ = 5): vehicle/control (WT-C), ANIT/control (WT-A), ANIT/fenofibrate 5, 25 and 125 mg·kg$^{-1}$ twice a day (WT-A-F5, WT-A-F25, WT-A-F125) and fenofibrate 5, 25 and 125 mg·kg$^{-1}$ twice a day (WT-F5, WT-F25, WT-F125). Considering that fenofibrate 25 mg·kg$^{-1}$ twice a day was found to totally inhibit the toxic responses, the *Pparα*-null mice were divided into four groups ($n$ = 5): vehicle/control (KO-C), ANIT/control (KO-A), ANIT/fenofibrate 25 mg·kg$^{-1}$ twice a day (KO-A-F25) and fenofibrate 25 mg·kg$^{-1}$ twice a day (KO-F25). Fenofibrate was dissolved in corn oil and administered by oral gavage twice daily for 5 days. A single dose of ANIT 75 mg·kg$^{-1}$ in corn oil was administered to the indicated groups on day 4.

To investigate the role of PPARα, wild-type mice were assigned to four groups: vehicle/control (WT-C), ANIT/control (WT-A), ANIT/WY14643 (WT-A-WY) and WY14643 (WT-WY). The WT-A-WY and WY14643 groups were fed a diet containing 0.1% (w·w$^{-1}$) WY14643 for 5 days. A single dose of ANIT 75 mg·kg$^{-1}$ in corn oil was administered to the indicated groups on day 4. To explore the role of the JNK pathway, wild-type mice were treated with the non-selective JNK pathway inhibitor SP600125. Specifically, four groups wild-type mice ($n$ = 5), vehicle/control (WT-C), ANIT/control (WT-A), ANIT/SP600125 15 mg·kg$^{-1}$ (WT-A-SP) and SP600125 15 mg·kg$^{-1}$ (WT-SP), were included in this experiment. To confirm whether JNK signalling was completely inhibited by the highest dose of fenofibrate, we used another four groups of wild-type mice, vehicle/control (WT-C), ANIT/control (WT-A), ANIT/fenofibrate 125 mg·kg$^{-1}$ twice a day (WT-A-F125) and ANIT/fenofibrate 125 mg·kg$^{-1}$/SP600125 (WT-A-F-SP). SP600125 was dissolved in corn oil and administered by i.p. injection once daily. Two hours after the first dose of SP600125, a single dose of ANIT 75 mg·kg$^{-1}$ was administered to the indicated groups.

Forty-eight hours after the administration of ANIT, the mice were weighed and killed by asphyxiation using carbon dioxide following blood collection. Liver tissues and gallbladder were harvested and weighed to determine changes in the liver and gallbladder. A section of freshly isolated liver tissue was excised and immediately fixed in 10% neutral buffered formalin after a brief wash with PBS. The remaining liver tissues were flash-frozen in liquid nitrogen and then stored at −80°C pending analysis.

To determine whether fenofibrate administration affects sclerosing cholangitis, we designed experiments to investigate the effects of this drug in a DDC-induced model of sclerosing cholangitis; the groups included wild-type vehicle/control (WT-C), DDC/control (WT-D) and DDC/fenofibrate 35 mg·kg$^{-1}$ (WT-D-F25). Sclerosing cholangitis was induced by DDC challenge for 7 days (Pollheimer and Fickert, 2015). Fenofibrate dissolved in corn oil was administered by oral gavage 3 days before DDC challenge. Twenty-four hours after the last dose of DDC and fenofibrate, the mice were killed and specimens were collected and analysed as above for protection phenotype.

## Assessment of serum levels of fenofibric acid

An aliquot of 30 μL serum was spiked into 60 μL of acetonitrile with bezafibrate as internal standard. The mixtures were vortexed for 30 s and centrifuged at −20°C and 15 000× $g$ for 20 min. The supernatant was analysed using a Shimadzu high-performance LC system (Kyoto, Japan) coupled with an API-4000 triple quadrupole mass spectrometer (Toronto, Canada).

## Biochemical analysis

Total bilirubin (TBIL), ALP, alanine aminotransferase (ALT), aspartate aminotransferase (AST), TBA and direct bilirubin (DBIL) in serum were assayed by the Spectra Max M5 (Molecular Devices, Sunnyvale, CA, USA). The analysis was carried out following the manufacturers' procedures described in the kits.

## Histopathological assessment

Fixed liver tissues in the above experiments were dehydrated in a serial concentrations of alcohol and xylene followed by paraffin embedding. Four-micrometre serial sections were cut and stained with haematoxylin and eosin. Histopathological examination was performed using an Olympus BX51 light microscope. Ten sections per preparation were analysed blindly by a pathologist.

## Quantitative PCR analysis

The total RNA from mouse hepatic tissues (20 mg) homogenized in Trizol reagent was determined by Multiskan Go (Thermo Scientific, Waltham, MA, USA). The reverse transcription system (20 μL) included the following items: 5 × Reaction buffer 4 μL, total RNA 1 μg, Oligo dT18 1 μL, Random primer 1 μL, 10 mM dNTPs Mix 2 μL, 200 U RevertAid M-MuLV RT 1 μL and 20 U Ribolock RNase inhibitor 1 μL. The cDNA synthesized was stored at −20°C and subjected to analysis within 7 days. The primer sequences, listed in Supporting Information Table S2, were extracted from http://mouseprimerdepot.nci.nih.gov. Each 10 μL PCR system contained 1 μL total cDNA, LightCycle 480 SYBR Green I Master Mix (FastStart Taq DNA polymerase, reaction buffer, dNTP mix, SYBR Green I dye, and $MgCl_2$) 5 μL, forward primer 0.2 μL, reverse primer 0.2 μL, nuclease-free water 3.6 μL. Amplification was performed

using reaction cycle at 95°C 10 s, 55°C 10 s and then 72°C 15 s. The fluorescence signal was detected at the end of each cycle. 18S rRNA was used as an internal control, and melting curve was used to confirm the specificity of the primers.

### Western blot analysis

Liver tissues were homogenized by MagNA Lyser (Roche, Indianapolis, IN, USA) using RIPA buffer (1:10, g/v) containing 1% PMSF (Shanghai, China). Tissue debris was removed by centrifugation at 10 000× *g* and 4°C for 5 min. The total protein was quantified using a BCA protein assay kit (Beyotime Biotech Co. Ltd, Nantong, China). An equivalent volume of 5X SDS-PAGE sample loading buffer (Shanghai, China) was added to the tubes that were then boiled for 5 min. The samples were loaded and separated on 10% SDS-polyacrylamide gels.

The samples were transblotted onto PVDF membranes which were blocked with 5% fat-free milk at 37°C for at least 2 h. Membranes were incubated overnight with primary antibodies against p-**MKK4** (phospho-mitogen-activated protein kinase kinase 4), t-MKK4 (total MMK4), p-JNK (phospho-JNK), t-JNK (total JNK), p-c-Jun (phospho-AP-1 transcription factor subunit), t-c-Jun (total c-Jun), t-p65, p-p65, p-STAT3 (phospho-STAT3), total STAT3 and GAPDH. After secondary antibody incubation for 1 h, the blotted membranes were exposed to ECL substrates (Advansta, Menlo Park, CA, USA) and the signals were detected by Tanon 4200SF (Tanon, Shanghai, China).

### Statistical analysis

The data and statistical analysis comply with the recommendations on experimental design and analysis in pharmacology (Curtis *et al.*, 2015). Data were presented as mean ± SD. The assignment of mice to different groups was randomized. The raw data were assessed independently by two co-authors to ensure the correctness of the conclusions. The investigators treating the mice were not aware of the pharmacological treatments of each group; each group was assigned a number during the assessment. Those who did the data analysis did not have access to the administration sheet. To detect a 25% change at a power 0.8 and $\alpha = 0.05$ with 8% SD, the effect required a minimum of five mice per group as calculated using GPOWER. The statistical analysis was performed using the software SPSS Statistics, version 23 (IBM, Beijing, China). Differences among multiple groups were tested using one-way ANOVA followed by Dunnett's *post hoc* comparisons. Comparison between ANIT/DDC and CON, A-F25/D-F25/A-WY/A-SP and CON groups in two mice lines were tested by Student's *t*-test. A difference was considered significant when $P < 0.05$ and was marked with an asterisk in the graphs accordingly.

### Materials

Fenofibrate was purchased from Shangqiu Chemry Chemicals Co. Ltd (Shangqiu, China). Fenofibric acid (FA), bezafibrate, ANIT, WY14643 and SP600125 were obtained from Sigma-Aldrich (St. Louis, MO, USA). TBA, ALP, ALT, AST, TBIL and DBIL assay kits were purchased from Yonghe Sunshine Technology (Changsha, China). Antibodies against p-MKK4 and t-MKK4, t-JNK and p-JNK, and p-c-Jun and t-c-Jun were purchased from Cell Signaling Technology (Danvers, MA, USA). Antibodies against p65 and the active form phospho-p65, total STAT3, p-STAT3 and GAPDH were acquired from Abcam (MA, USA). The reverse transcription kit and LightCycle 480 SYBR Green I Master Mix were obtained from Roche Diagnostics (Mannheim, Germany). All the other chemicals were of the highest grade available from commercial sources.

### Nomenclature of targets and ligands

Key protein targets and ligands in this article are hyperlinked to corresponding entries in http://www.guidetopharmacology.org, the common portal for data from the IUPHAR/BPS Guide to PHARMACOLOGY (Southan *et al.*, 2016), and are permanently archived in the Concise Guide to PHARMACOLOGY 2015/16 (Alexander *et al.*, 2015a,b,c).

## Results

### Pharmacokinetics of fenofibrate administration to mice

A calibration curve was constructed using authentic FA and the negative ion transition m/z 317.1/231 for FA was detected in multiple reactions monitoring mode (Supporting Information Figure S1A). The plasma concentration of FA in groups WT-F5, WT-F25 and WT-F125 treated with fenofibrate were 0.16 ± 0.04, 1.24 ± 0.49 and 5.40 ± 0.95 $\mu g \cdot mL^{-1}$ respectively (Supporting Information Table S1). However, in the WT-A-F5, WT-A-F25 and WT-A-F125 groups, the FA concentrations were 0.83 ± 0.43, 0.96 ± 0.81 and 1.90 ± 1.29 $\mu g \cdot mL^{-1}$ respectively. Similar to the concentrations of the WT-F-25 group, the FA levels in the KO-A-F25 and KO-F-25 groups were 0.94 ± 0.47 and 0.88 ± 1.74 $\mu g \cdot mL^{-1}$. The FA concentration in the WT-A-F5 group was higher than that in the WT-F5 group, and the concentration in the WT-A-F125 group was lower than that in the WT-F125 group (Supporting Information Figure S1B). Based on a linear pharmacokinetic model, the dose of fenofibrate in humans producing the similar trough concentration as that in WT-A-F25 was estimated to be only 1/4–1/3 of the present dose for atherosclerosis (Supporting Information Table S1).

### Fenofibrate protected against ANIT-induced cholestasis and liver injury

In the wild-type mice, serum ALP, TBA, TBIL, DBIL, ALT and AST were significantly increased in the ANIT group compared with the WT-C group ($P < 0.05$; Figure 1). In the WT-A-F25, but not WT-A-F5 or WT-A-F125 mice, the above indicators were totally inhibited compared with the WT-A group ($P < 0.05$). Wild-type mice treated with fenofibrate (WT-F5, WT-F25 and WT-F125) showed no hepatotoxicity. In the *Pparα*-null mouse groups, ALP, TBA, TBIL, DBIL ALT and AST were significantly increased in the KO-A group compared with the KO-C group ($P < 0.05$), which was similar to that in the WT-A group. However, the biochemical indicators in the KO-A-F25 group pretreated with fenofibrate at 25 $mg \cdot kg^{-1}$ twice a day were not inhibited compared with those in the KO-A group (Figure 1). Pathological analysis of the hepatic tissues in both the WT-C and KO-C groups exhibited normal histology (Figure 2A). The WT-A group exhibited a loss of cellular boundaries, degenerative changes and marked necrosis

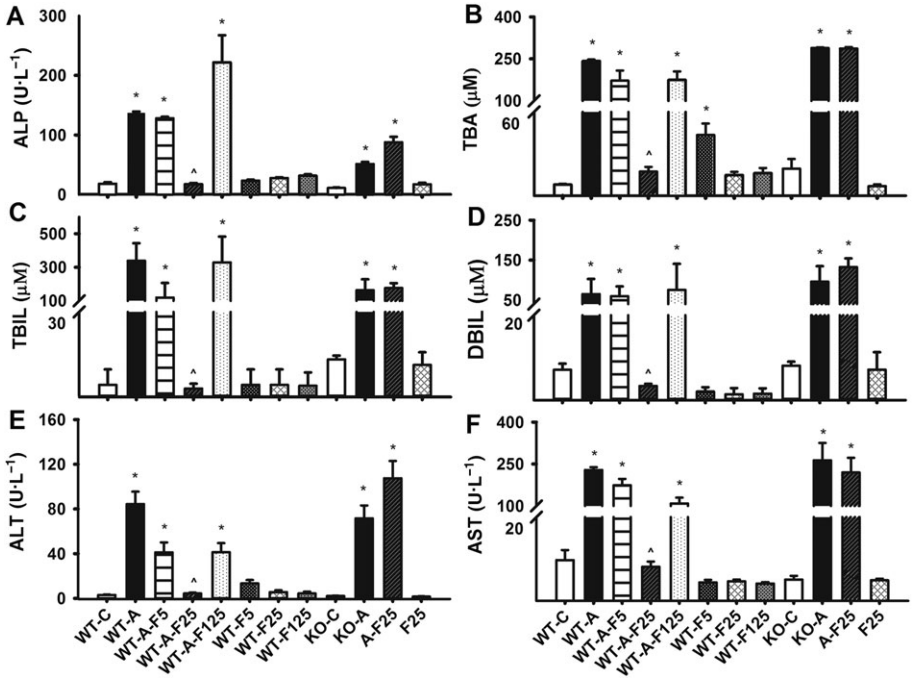


## Figure 1

Biochemical markers indicating the protective effect of fenofibrate against intrahepatic cholestasis. (A) ALP in wild-type and *Ppara*-null mice respectively. (B) TBA in wild-type and *Ppara*-null mice. (C) TBIL in wild-type and *Ppara*-null mice. (D) DBIL in wild-type and *Ppara*-null mice. (E) ALT in wild-type and *Ppara*-null mice. (F) AST in wild-type and *Ppara*-null mice. The data are expressed as mean ± SD ($n = 5$, * $P < 0.05$, compared with WT-C/KO-C; ^ $P < 0.05$, compared with WT-A/KO-A).

(Figure 2B). Similar destruction was observed in the WT-A-F5 and WT-A-F125 groups. In contrast, no pathological change was noted in the WT-F25 group (Figure 2D). In the *Pparα*-null mice, the liver injury was similar between the KO-A-F25 and KO-A groups (Figure 2F, G). Thus, pretreatment with fenofibrate protected mice against the ANIT-induced liver injury, and this effect was dependent on both fenofibrate dose and PPARα activation.

## *Bile acid metabolism and transport were adaptively modified*

ANIT challenge decreased *Cyp7a1* and *Cyp8b1* mRNA levels in wild-type and *Pparα*-null mice compared with the control groups ($P < 0.05$). In the WT-A-F5, WT-A-F125, KO-A and KO-A-F25 groups, *Cyp7a1* and *Cyp8b1* mRNA levels were decreased similarly compared with WT/KO-C groups. However, in the WT-F25 group, *Cyp7a1* and *Cyp8b1* mRNA levels were significantly increased compared with the WT-A group ($P < 0.05$), similar to the WT-C ($P > 0.05$) group (Figure 3 A–C). In contrast, *Mdr2* (*Abcc2*) mRNA was significantly increased in the WT-A group compared with the WT-C ($P < 0.05$), and these changes could be modified by fenofibrate in the A-F25 group. In the three wild-type groups treated with fenofibrate, *Mdr2* mRNA was significantly increased in the WT-F5, WT-F25 and WT-F125 groups compared with the WT-C group ($P < 0.05$), and no modification of *Cyp7a1* and *Cyp8b1* mRNA was observed.

**Organic anion-transporting polypeptide 1 (OATP1** also known as OATP1C1**)** and multidrug resistance-related protein 4 (**MRP4**) are involved in the efflux of bile acids. Levels of *Oatp1*, *Mrp3* and *Mrp4* mRNA were modified by fenofibrate in a dose-dependent manner ($P < 0.05$). *Oatp1* mRNA was significantly decreased in the two ANIT-treated groups in two mouse lines ($P < 0.05$), as well as the cholestatic groups WT-A-F5, WT-A-F125, KO-A and KO-A-F25. But *Oatp1* mRNA level were also decreased in the WT-A-F25 group compared with the WT-C or WT-A group ($P < 0.05$; Figure 3D). *Mrp3* and *Mrp4* mRNA was increased in ANIT-treated mice, and the WT-A-F5, WT-A-F125, KO-A and KO-A-F25 cholestatic groups when compared with the WT/KO-C group ($P < 0.05$). In the WT-A-F25 group, *Mrp3* mRNA level was unchanged compared with the WT-C group, but *Mrp4* mRNA was significantly increased ($P < 0.05$). Changes in expression of *Oatp1* and *Mrp4* mRNAs in the WT-A-F25 non-cholestatic group probably occurred because they were regulated by both bile acid feedback and fenofibrate action (Figure 3D–F).

**BSEP** (bile salt export pump also known as ABCB11) and **OSTB** (heteromeric organic solute transporter-β) are also involved in efflux bile acids. Neither of them was modified by fenofibrate, but both of their mRNAs were significantly increased in the two ANIT-treated groups and the WT-A-F5, WT-A-F125, KO-A and KO-A-F25 cholestatic groups ($P < 0.05$). Both mRNAs were unchanged in the WT-A-F25 non-cholestatic group. In comparison with moderate changes in levels of *Bsep* mRNA (2.8–5.2-fold), *Ostb* mRNA was sharply increased, suggesting different sensitivity to bile acid feedback and the potential contribution to bile acid detoxification (Supporting Information Figure S2A-D).

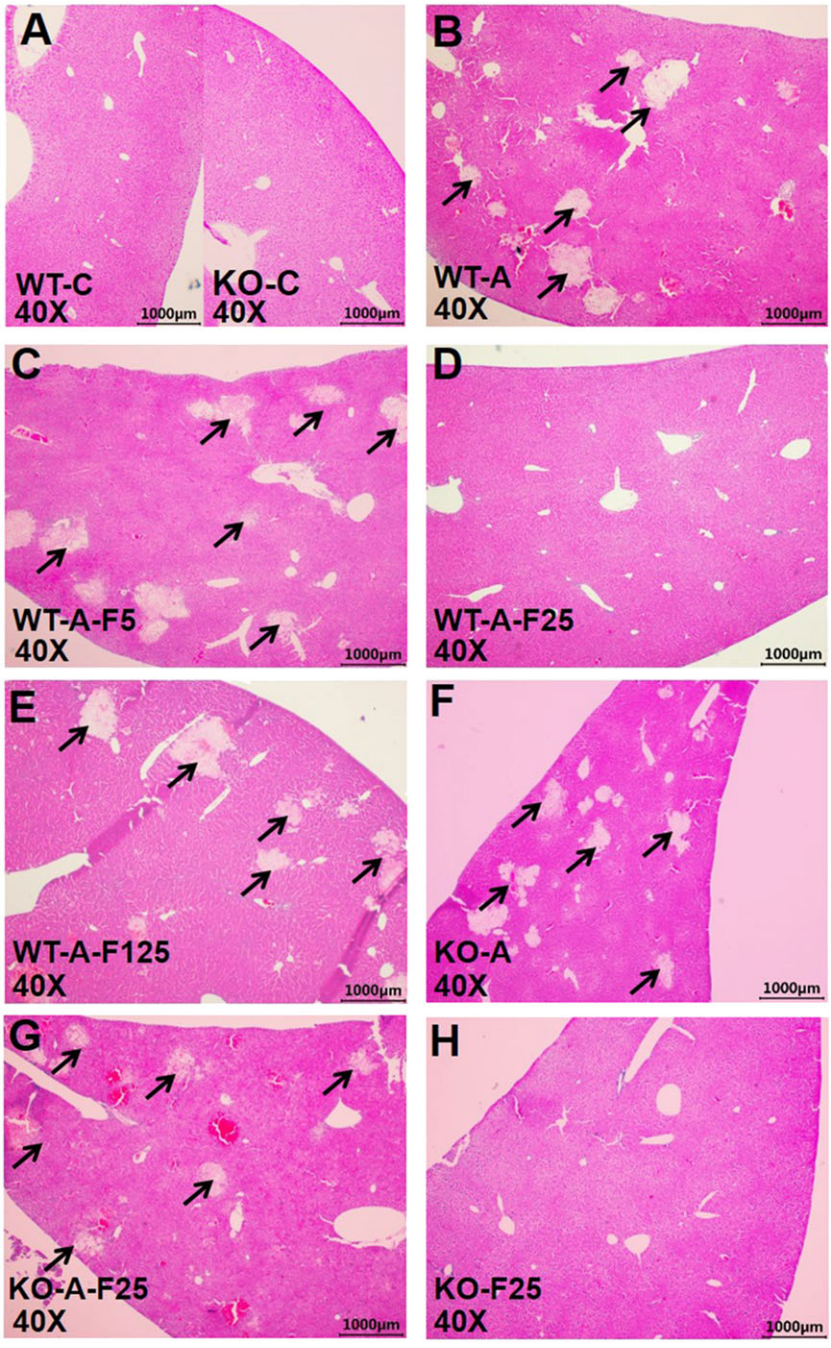


## Figure 2

Histopathological analysis of liver tissues indicating the liver injury and the protective role of fenofibrate in intrahepatic cholestasis. (A) Haematoxylin and eosin (HE) staining of liver tissues in the WT-C and KO-C groups. (B) HE staining of liver tissues in the WT-A group. (C, D, E) HE staining of liver tissues in the WT-A-F5, WT-A-F25 and WT-A-F125 groups respectively. (F) HE staining of liver tissues in the KO-A group. (G, H) HE staining of liver tissues in the KO-A-F25 and KO-F25 groups respectively. Arrows: exhibited a loss of cellular boundaries, degenerative changes and marked necrosis.

### *NF-κB, STAT3 and JNK pathways were differently activated*

In wild-type mice, *Il-1β* mRNA was significantly increased in the cholestatic WT-A, WT-A-F5 and WT-A-F125 groups compared with the WT-C group ($P < 0.05$; Figure 4A). In KO-A, KO-A-F25 and KO-F25 groups, it was significantly increased compared with KO-C group ($P < 0.05$; Figure 4B). Increased *Il-6* mRNA was not observed in the wild-type groups except for a moderate increase in the WT-A-F5 group. *Il-6* mRNA was significantly increased in the KO-A, KO-A-F25 and KO-F25 groups compared with the KO-C group ($P < 0.05$; Figure 4C, D). The *Il-10* encoding the protective cytokine

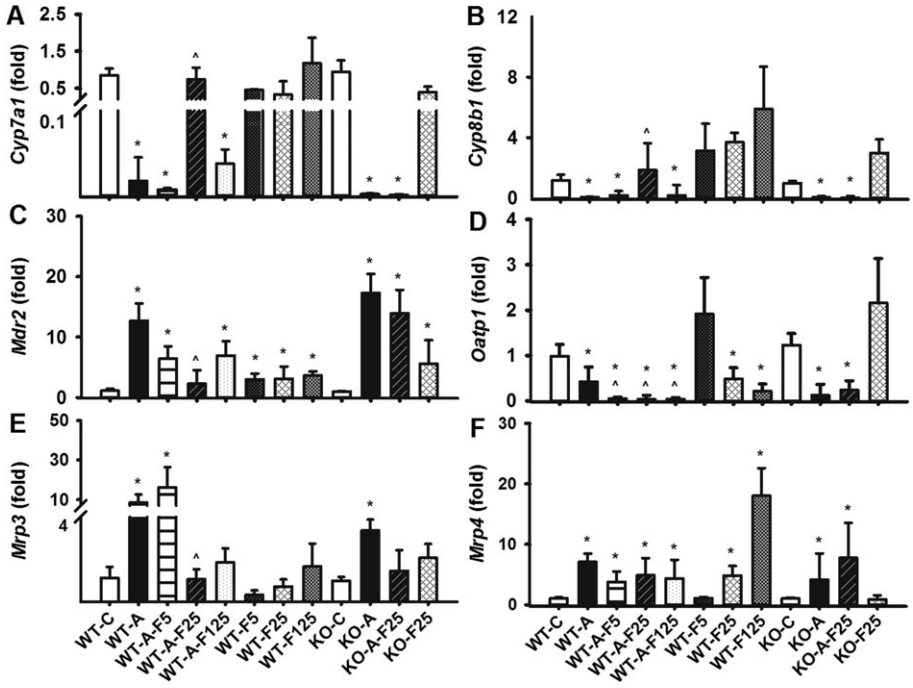


## Figure 3

Different effects of fenofibrate on the expression of genes involved in bile acid metabolism and transport. (A) *Cyp7a1* mRNA level in wild-type and *Ppara*-null mice. (B) *Cyp8b1* mRNA in wild-type and *Ppara*-null mice. (C) *Mdr2* mRNA level in wild-type and *Ppara*-null mice. (D) *Oatp1* mRNA level in wild-type and *Ppara*-null mice respectively. (E) *Mrp3* mRNA level in wild-type and *Ppara*-null mice respectively. (F) *Mrp4* mRNA level in wild-type and *Ppara*-null mice respectively. The mRNA levels were measured by quantitative PCR and normalized by *18S rRNA*. mRNA levels in the vehicle-treated control mice were set as 1 and the results expressed as mean ± SD ($n = 5$, * $P < 0.05$, compared with WT-C/KO-C; ^ $P < 0.05$, compared with WT-A/KO-A).

IL-10 was significantly increased in the WT-A group among all the wild-type groups ($P < 0.05$). *Il-10* mRNA was significantly increased in the KO-A, KO-A-F25 and KO-F25 groups compared with the KO-C group ($P < 0.05$; Figure 4E, F). *Tnf-α* was not modified in the wild-type groups, but it was increased by only threefold to fivefold in the KO-A and KO-A-F25 groups compared with the KO-C group. These data indicated that increased inflammation occurred in the cholestatic groups, but it was unclear which of the above factors triggered the inflammation.

A dose-dependent inhibition of p-p65 was clearly observed in all groups treated with fenofibrate (Figure 4G). However, its inhibition was not observed in the *Pparα*-null groups. Activation of p-STAT3 was observed in both wild-type and *Pparα*-null mice, but was more pronounced in the latter group (Figure 4G). The STAT3 target gene mRNAs suppressor of cytokine signalling 3 (*Socs3*), fibrinogen α chain, fibrinogen β chain and fibrinogen γ chain were up-regulated less than fourfold in the wild-type groups. In the KO-A and KO-A-F25 cholestatic groups, their expression was increased by 14- and 15-fold, 15- and 16-fold, 12- and 12-fold and 26- and 16-fold respectively ($P < 0.05$; Supporting Information Figure S3). Thus, the fenofibrate-inhibited NF-κB-STAT3 signalling was dependent on PPARα. However, the inhibition neither correlated with nor contributed to inhibition of cholestasis or hepatic injury in the two mouse lines.

Compared with the WT-C group, the *c-Jun* and *c-Fos* mRNAs were significantly increased in the WT-A, WT-A-F5, WT-A-F125 and WT-F125 groups ($P < 0.05$), but not in the WT-A-F25 group compared with the WT-C group (Figure 5A, C). In *Pparα*-null mice, the *c-Jun* and *c-Fos* mRNAs were significantly increased in the KO-A and KO-A-F25 groups ($P < 0.05$; Figure 5B, D). The Western blot analysis showed that p-MKK4 was activated in the WT-A and WT-A-F5 groups but was inhibited in the WT-A-F25 and WT-A-F125 groups (Figure 5E). p-JNK was activated in the WT-A and WT-A-F5 groups, totally inhibited in the WT-A-F25 group, but only partly inhibited in WT-A-F125 group. In the *Pparα*-null mice, activation of p-MKK4 was not evident, but p-JNK was increased more in the three experimental groups than in the KO-C group (Figure 5E). Activation p-c-Jun was observed in all the cholestatic groups of the two mouse lines but was not in the WT-A-F25 and KO-F25 groups in which cholestasis was totally inhibited or did not occur (Figure 5E). Thus, the JNK pathway might contribute to cholestasis or hepatic injury in the two mouse lines.

### *WY14643 inhibited cholestatic liver injury and this was associated with JNK inhibition*

In wild-type mice, serum TBA, ALT, TBIL and DBIL levels were significantly increased respectively in the WT-A group ($P < 0.05$). In WT-A-WY mice, the above indicators were totally inhibited (Figure 6A–D). The WT-A group exhibited

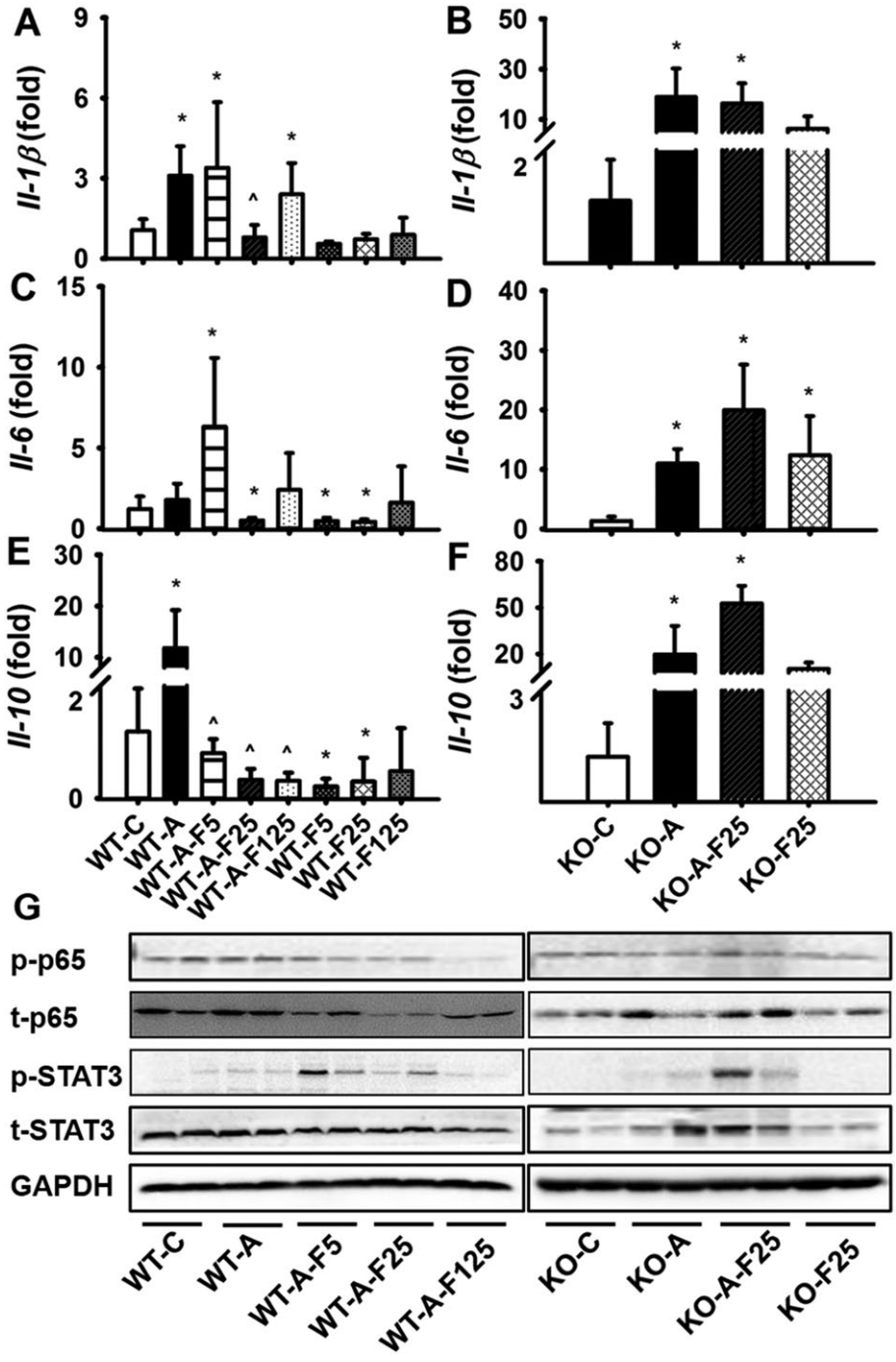


## Figure 4

Effects of fenofibrate on the expression of inflammatory and anti-inflammatory factors associated with NF-κB and STAT3 signalling. (A, B) *Il-1β* mRNA levels in the wild-type and *Ppara*-null mice. (C, D) *Il-6* mRNA levels in the wild-type and *Ppara*-null mice. (E, F) *Il-10* mRNA levels in the wild-type and *Ppara*-null mice respectively. The mRNA levels were measured by Q-PCR and normalized by *18S rRNA*. mRNA levels in the vehicle-treated control mice were set as 1 and the results expressed as mean ± SD ($n$ = 5, * $P < 0.05$, compared with WT-C/KO-C; ^ $P < 0.05$, compared with WT-A/KO-A). (G) Western blot analysis of NF-κB and STAT3 signalling mediated by PPARα. Data were from liver samples collected 5 days after fenofibrate treatment, and 2/5 of the liver tissues were randomly selected for Western blot analysis. GAPDH was used as a loading control.

a loss of cellular boundaries, degenerative changes and marked necrosis. In contrast, no obvious alteration of liver histology was observed in the WT-A-WY and WT-WY group (Figure 6E), indicating a protective effect. The JNK pathway was activated in WT-A group and totally inhibited in the WT-A-WY group (Figure 6E).

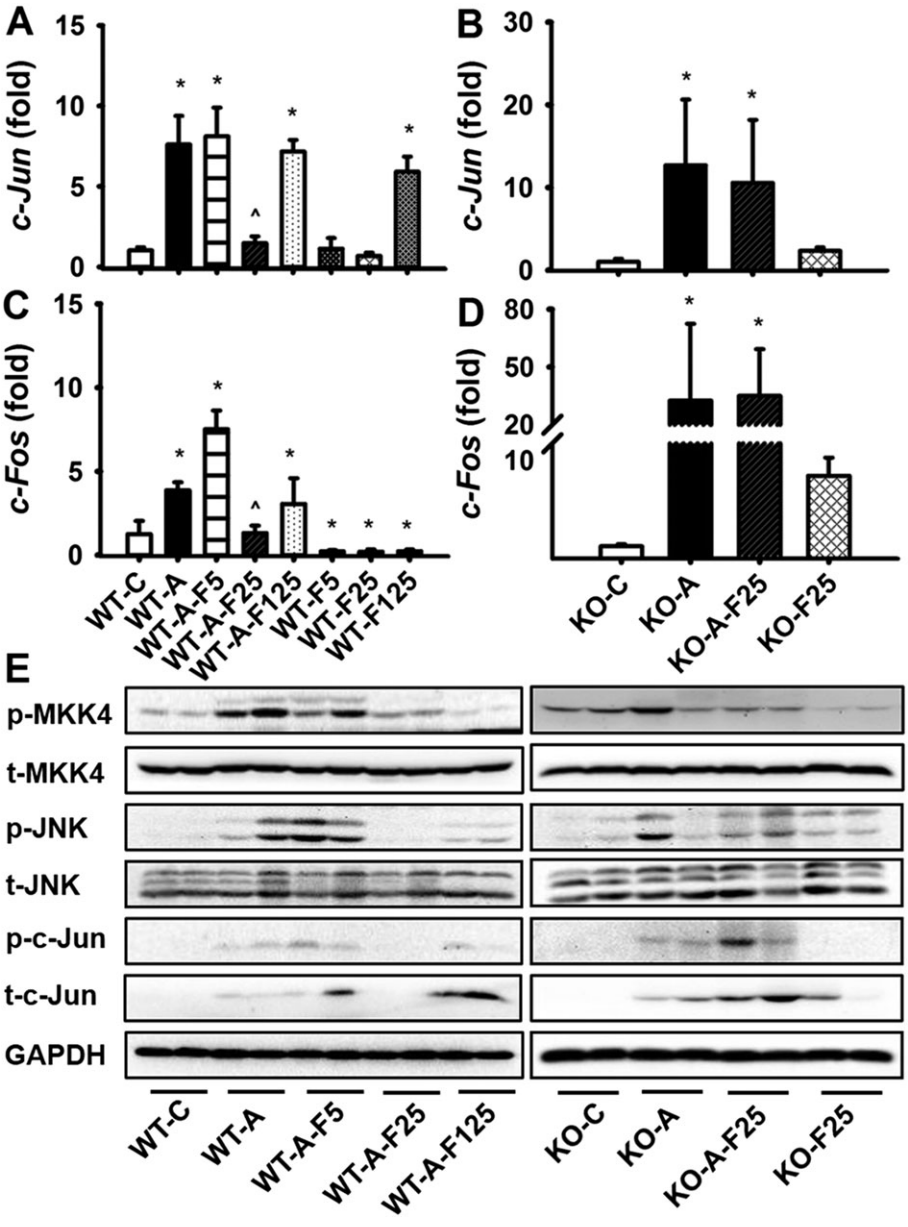


## Figure 5

Inhibition of the JNK pathway is involved in fenofibrate and PPARα-mediated protection. (A, B) *c-Jun* mRNA level in wild-type and *Ppara*-null mice. (C, D) *c-Fos* mRNA level in wild-type and *Ppara*-null mice respectively. (E) Western blots of components of the JNK signalling pathway in liver extracts. The mRNA levels were measured by Q-PCR and normalized by *18S* rRNA. mRNA levels in the vehicle-treated control mice were set as 1 and the results expressed as mean ± SD. For Western blot analysis, the data were from liver samples collected 5 days after fenofibrate treatment, and two were randomly selected for protein analysis. ($n = 5$, * $P < 0.05$, compared with WT-C/KO-C; ^ $P < 0.05$, compared with WT-A/KO-A).

### *JNK inhibitor SP600125 blocked ANIT-induced cholestatic liver injury*

In comparison with the WT-A group, the ALP, TBA, TBIL and DBIL levels in WT-A-SP were not modified, suggesting that cholestasis occurred even after treatment with SP600125. However, the ALT and AST level in the WT-A-SP group was significantly decreased, indicating that cholestatic liver injury was inhibited (Figure 7A–F). Pathological analysis revealed no obvious alterations in liver histology in the WT-A-SP and WT-SP groups (Figure 7G), which confirmed a definite protective effect of SP600125. The JNK pathway was inhibited in the WT-SP-A group compared with the WT-A group as indicated by the level of p-JNK and p-c-Jun (Figure 7H). This effect was similar to that observed in the WT-A-F25 and the WT-A-WY group. These data indicate that the JNK pathway mediates the cholestatic liver injury, and its inhibition results in the attenuation of cholestatic liver injury by PPARα agonists.

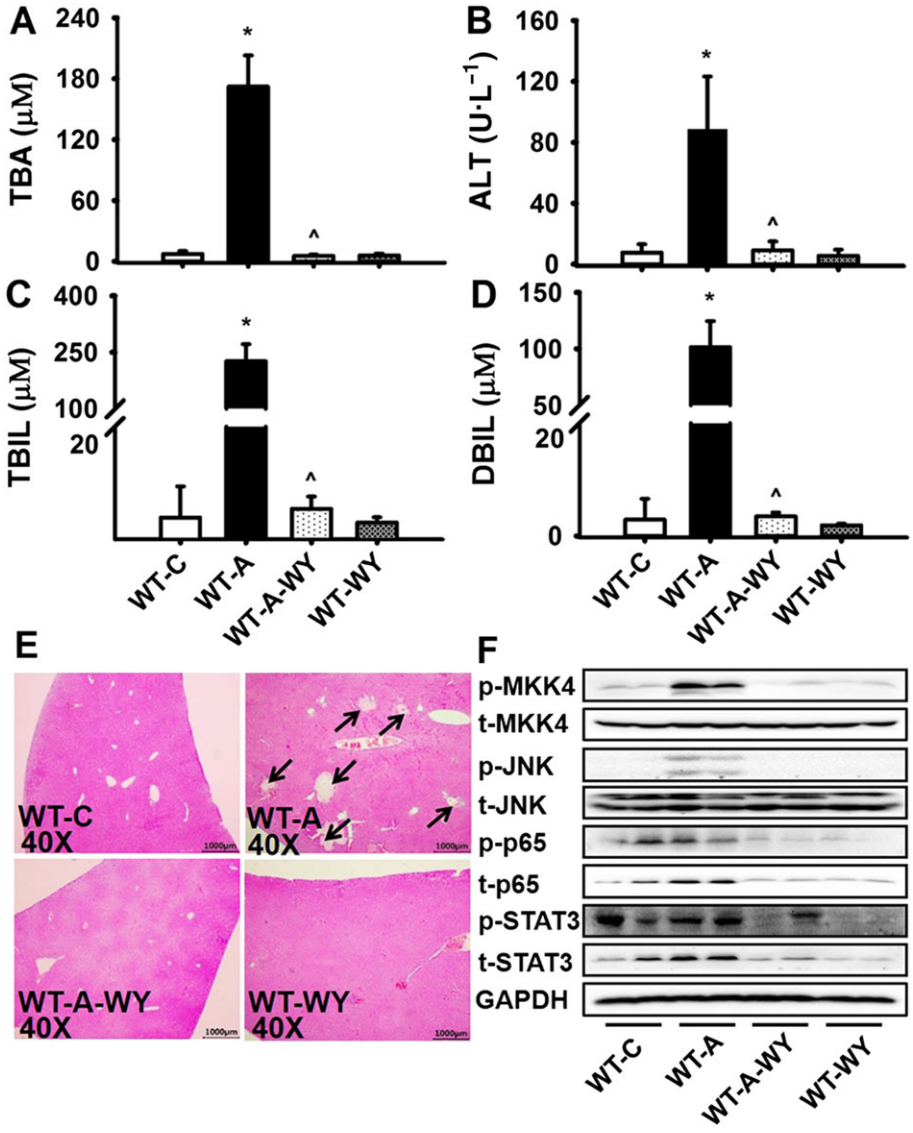


## Figure 6

WY14643 affects ANIT-induced cholestasis and liver injury. (A–D) Typical biochemical markers TBA, ALT, TBIL and DBIL indicate the protective effect of WY14643 against cholestatic liver injury. (E) Histopathological analysis of liver tissues indicating the protective role of WY14643 in intrahepatic cholestasis. (F) Western blots of JNK, NF-κB and STAT3 signalling pathways in liver extracts. The data are expressed as mean ± SD ($n = 5$, * $P < 0.05$,compared with WT-C; ^ $P < 0.05$, compared with WT-A). Arrows: indicate a loss of cellular boundaries, degenerative changes and marked necrosis.

### *SP600125 inhibited cholestatic liver injury in the WT-A-F125 group*

In comparison with the WT-A and WT-A-F125 group, the ALP, TBA, TBIL and DBIL levels in the WT-A-F-SP group were not modified, suggesting cholestasis occurred even though the mice had been treated with SP600125. However, the ALT and AST levels in the WT-A-F-SP group were significantly decreased, indicating that cholestatic liver injury was inhibited (Figure 8A–F). Pathological analysis revealed no alterations in liver histology in the WT-A-F-SP group (Figure 8G), which confirmed the protective effect of SP600125 and fenofibrate. The JNK pathway was inhibited in the WT-A-F-SP group compared with the WT-A and WT-A-F125 group as indicated by the level of p-JNK (Figure 8H). This was similar to that of the WT-A-F25 group and the WT-A-WY group. These data corroborated the involvement of JNK signalling in cholestatic liver injury and confirmed that incompletely inhibited JNK signalling mediated the hepatic injury in the WT-A-F125 group.

### *Fenofibrate protected against DDC-induced sclerosing cholangitis*

In comparison with the WT-C group, the ALP, TBA, ALT, AST, TBIL and DBIL levels in the WT-D group were significantly increased. However, the ALP, TBA, ALT, AST, TBIL and DBIL

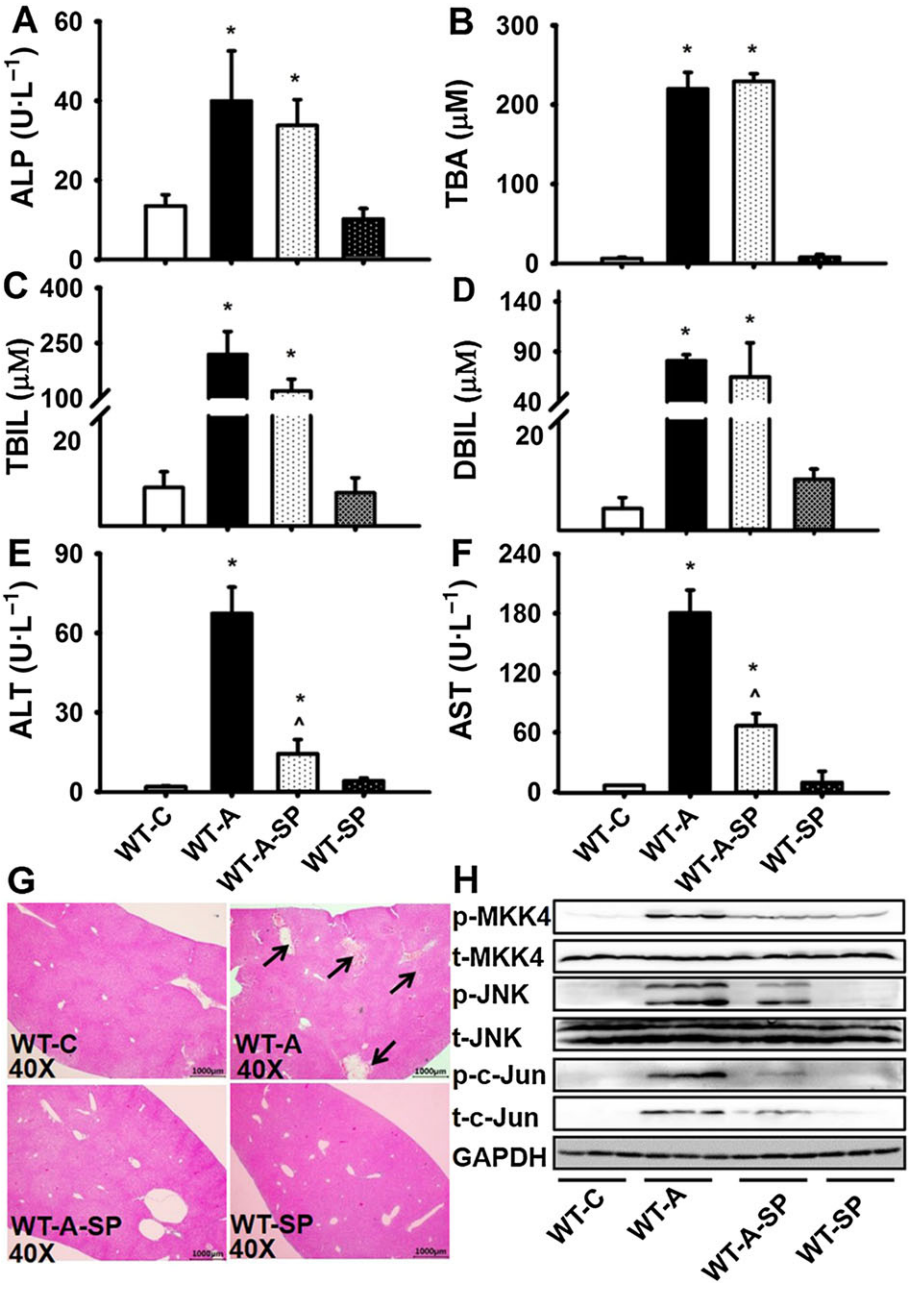


## Figure 7

SP600125 blocks ANIT-induced cholestatic liver injury. (A–F) Biochemical markers indicate the protective effect of SP600125 against liver injury. (G) Histopathological analysis of liver tissues indicating the inhibitory role of SP600125 in cholestatic liver injury. (H) Western blots of components of the JNK signalling pathway in liver extracts. The data are expressed as mean ± SD ($n = 5$, * $P < 0.05$, compared with WT-C; ^ $P < 0.05$, compared with WT-A). Arrows: indicate a loss of cellular boundaries, degenerative changes and marked necrosis.

levels in the WT-D-F25 group were not modified, indicating that cholestatic liver injury was inhibited by fenofibrate (Figure 9A–F). DDC feeding leads to ductular proliferation and cholangitis with onion skin type-like periductal fibrosis in WT-D group mice. No obvious alteration of the liver histology was observed in the WT-D-F25 group (Figure 9G), which confirmed a definite protective effect of fenofibrate. This result suggests that fenofibrate is also an effective treatment for sclerosing cholangitis.

## Discussion

Clinically, fenofibrate is prescribed at doses of 150–300 mg·day$^{-1}$ for dyslipidaemia (Shirinsky *et al.*, 2013; Harmer *et al.*, 2015; Masana *et al.*, 2015). In monotherapy or in combination with UDCA, the fenofibrate dose for cholestatic liver diseases is usually between 100 and 200 mg·day$^{-1}$ (Nakamuta *et al.*, 2005; Walker *et al.*, 2009; Levy *et al.*, 2011). According to the transition method based on body surface

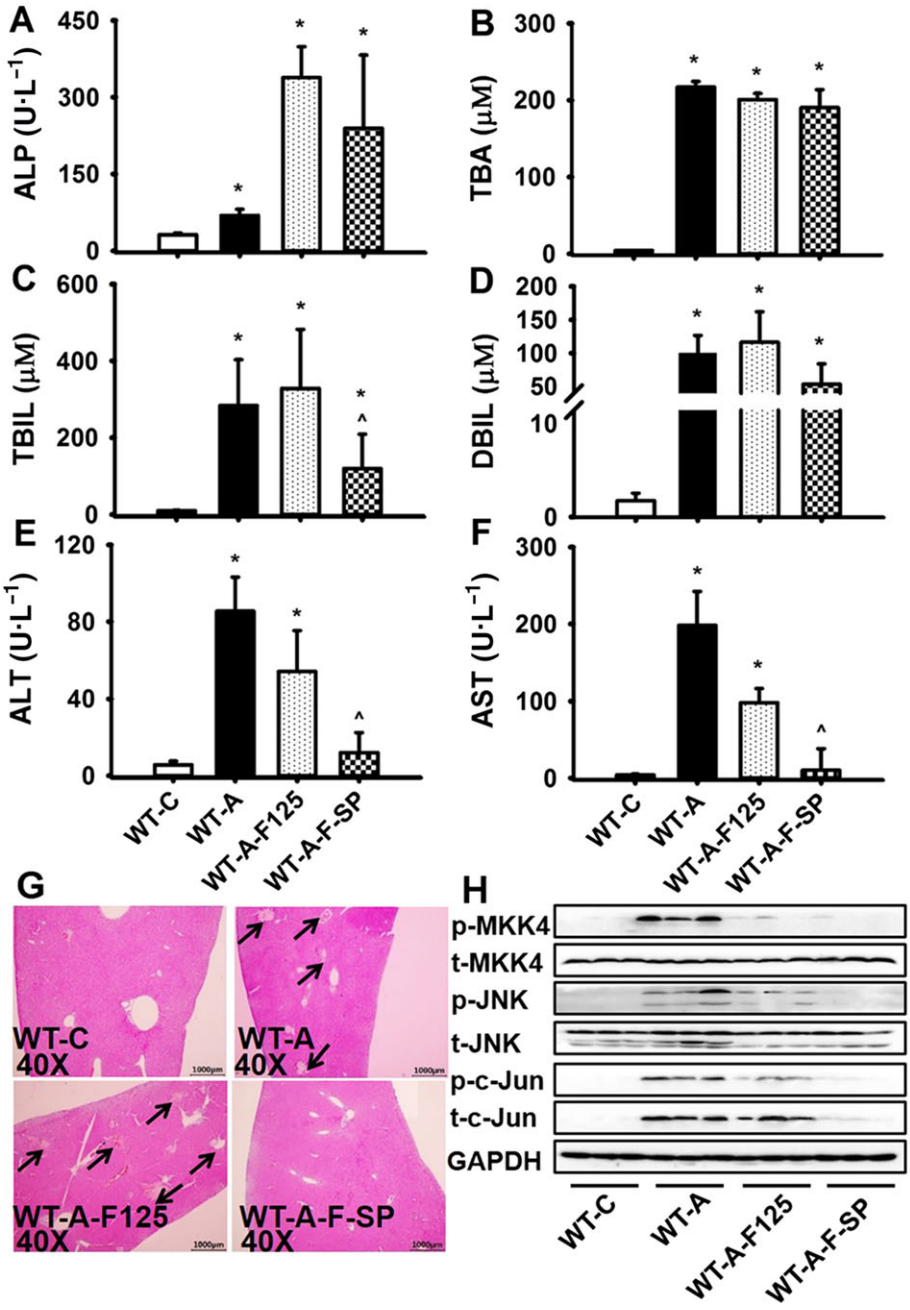


## Figure 8

SP600125 inhibits ANIT-induced cholestatic liver injury in the WT-A-F125 group. (A–F) Biochemical markers indicate the protective effect of SP600125 against liver injury. (G) Histopathological analysis of liver tissues indicating the inhibitory role of SP600125 in cholestatic liver injury. (H) Western blots of components of the JNK signalling pathway in liver extracts. The data are expressed as mean ± SD ($n = 5$, * $P < 0.05$, compared with WT-C; ^ $P < 0.05$, compared with WT-A). Arrows: indicate a loss of cellular boundaries, degenerative changes and marked necrosis.

area, the equivalent dose in mice is 22.5–45 mg·kg$^{-1}$. In a mouse nonalcoholic steatohepatitis model, fenofibrate at 50 mg·kg$^{-1}$·day$^{-1}$ improved obesity, dyslipidaemia, liver dysfunction and NASH pathology (Honda *et al.*, 2017). In rodent models, fenofibrate at 100 and 200 mg·kg$^{-1}$·day$^{-1}$ partially improved ALP, γ-glutamyl transferase, TBA, ALT, AST, TNF-α and IL-1β levels (Cindoruk *et al.*, 2007; El-Sisi *et al.*, 2013). Two preliminary experiments conducted in this study found the critical dose range was 5–125 mg·kg$^{-1}$ twice daily.

In the present study, fenofibrate at 25 mg·kg$^{-1}$ twice a day totally inhibited cholestasis but at 0.2- or 5-fold of the above dose it was ineffective, indicating that protection was dependent on fenofibrate dose. In human hepatocytes, the fenofibrate effect on MDR3 was dose-dependent between 12.5 and 50 μM. However, the effect was reduced when the concentration was increased to 125 μM (Ghonem *et al.*, 2014). It is reasonable to suggest that drugs at high doses may trigger some unknown factors that cause liver toxicity.

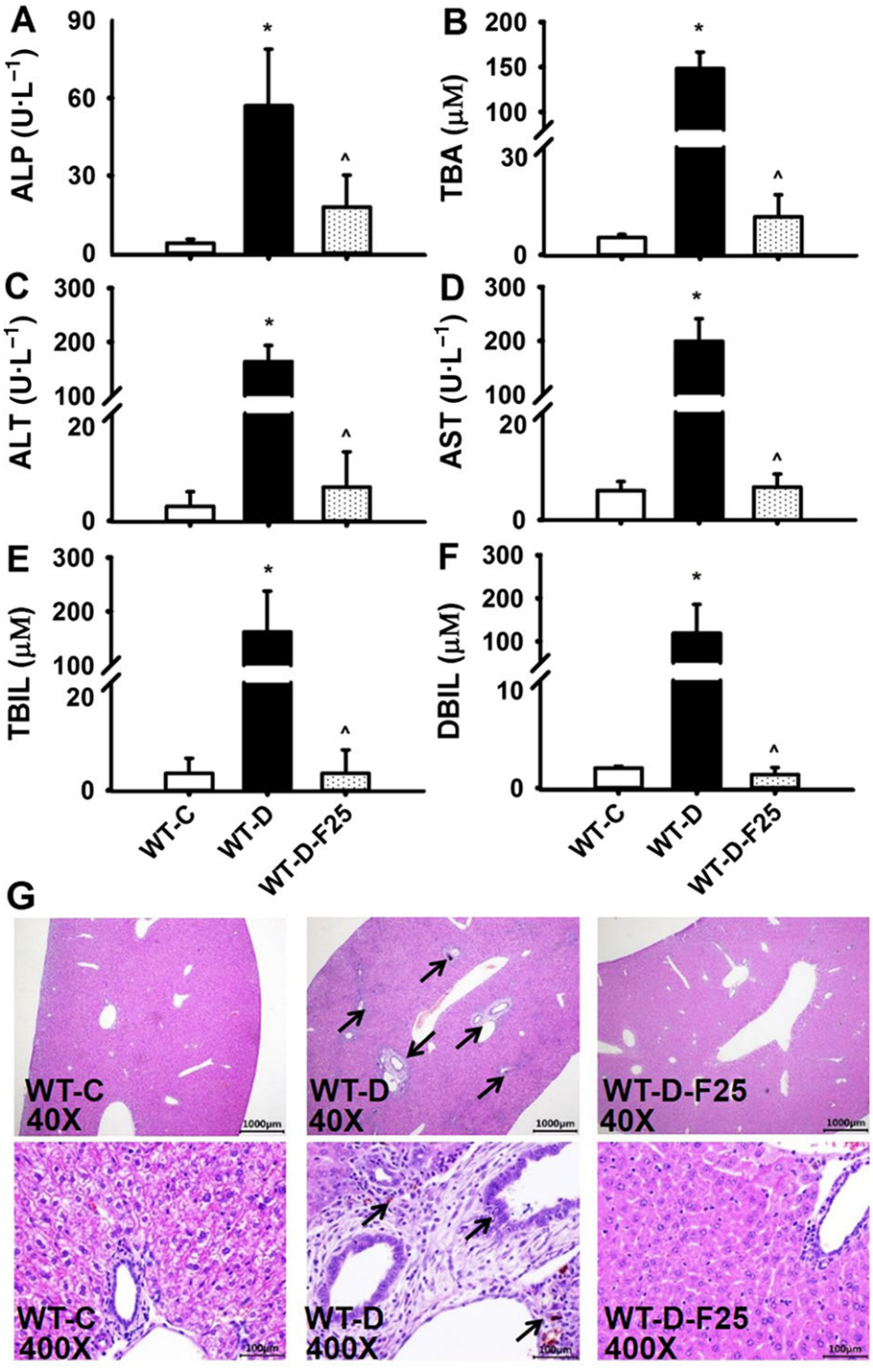


## Figure 9

Fenofibrate inhibits DDC-induced cholestatic liver injury in the WT-A-F125 group. (A–F) Biochemical markers indicate the protective effect of fenofibrate 25 mg·kg$^{-1}$ against DDC-induced cholestatic liver injury. (G) Histopathological analysis of liver tissues indicating the inhibitory role of fenofibrate 25 mg·kg$^{-1}$ in DDC-induced cholestatic liver injury. The data are expressed as mean ± SD ($n$ = 5, * $P < 0.05$, compared with WT-C; ^ $P < 0.05$, compared with WT-A). Arrows: indicate ductular proliferation and cholangitis with onion skin type-like periductal fibrosis.

Fenofibrate 125 mg·kg$^{-1}$ twice a day was associated with incomplete inhibition of the JNK pathway. However, SP600125 was found to inhibit the hepatic injury in the WT-A-F125 group, suggesting that the lower efficacy of fenofibrate at 125 mg·kg$^{-1}$was due to incomplete inhibition of JNK signalling.

At the steady state of fenofibrate in the clinic, the $C_{ss\ max}$ of FA is 9.0–9.6 μg·mL$^{-1}$ under different regimens and the

$C_{ss\ min}$ is 3.2–5.85 μg·mL$^{-1}$ (Table 1) (Martin *et al.*, 2003; Bergman *et al.*, 2004). In the present study, the $C_{ss\ min}$ of FA showed evidence of dose-dependence. The $C_{ss\ min}$ in the protected group treated with fenofibrate 25 mg·kg$^{-1}$ twice a day was 1.24 ± 0.49 μg·mL$^{-1}$, which was only 1/5 to 2/5 of the FA $C_{ss\ min}$ level in humans. If this exposure level was also the most effective for humans, the calculated dose in humans could be between 42 ± 9.1 and 62 ± 9.4 mg·day$^{-1}$ based on linear pharmacokinetics (Supporting Information Table S1). This dose range of fenofibrate was much lower than the specified doses for dyslipidaemia in the clinic. Thus, the dose–exposure–response relationship found in this study raises an interesting question: is it necessary and is it worth performing clinical trials to determine whether a lower fenofibrate dose produces better anti-cholestatic effects?

Bile acid homeostasis depends on the balance among synthesis, uptake and basolateral and canalicular export of bile acids. In this study, mRNAs encoded by genes involved in increasing bile acid level in hepatocytes, *Cyp7a1*, *Cyp8b1* and *Oatp1*, were all down-regulated in the cholestatic groups, while *Cyp7a1*and *Cyp8b1* mRNAs were unchanged in the WT-A-F25-protected group. In contrast, *Oatp1* mRNA was also down-regulated in the WT-A-F25 group because it was also affected by fenofibrate. This effect was in accord with that previously reported for MDR2, MRP3, MRP4, BSEP and OSTB, which are responsible for decreasing bile acid levels in hepatocytes (Kok *et al.*, 2003). Their mRNA expression patterns showed a tendency to be increased in all cholestatic groups, but were unchanged in the WT-A-F25 group. An exception was *Mrp4* mRNA that was also increased in the WT-A-F25 group, because it was also affected by fenofibrate. This effect is in agreement with the increases in *Mrp4* mRNA and protein expression induced by clofibrate observed previously (Delerive *et al.*, 2000). Considering the above common reactions, the effects of fenofibrate on the synthesis, uptake and export of bile acids are likely to be mainly adaptive responses, in agreement with an earlier perspective (Pogson *et al.*, 1999; Yang *et al.*, 2012). Only the pharmacological regulation of *Oatp1* and *Mrp4* mRNA seemed to contribute to the detoxification effects of fenofibrate. This contrasts with a previous suggested mechanism that CYP7A1 and MDR3 are involved in the anti-cholestatic effect of fenofibrate (Ghonem *et al.*, 2015).

NF-κB activation leads to an increase in inflammatory factors including TNF-α, IL-1 and IL-6. And TNF-α in turn can activate NF-κB signalling (Sarma *et al.*, 2014). NF-κB is involved in hepatotoxicity and protection against hepatotoxins can be mediated by inhibiting NF-κB signalling (Liu *et al.*, 2014b; Tan *et al.*, 2016). The PPARα agonists FA, ciprofibrate and WY14643 inhibit p65-mediated activation of *Il-1β* by inducing the inhibitory IκBα in human aortic cells (Delerive *et al.*, 2000). In human endothelial cells, fenofibrate and WY14643 reduced the promoter activity of vascular cell adhesion molecule 1 (VCAM1) by inhibiting the NF-κB pathway (Marx *et al.*, 1999). Thus, NF-κB was thought to be involved in the anti-cholestatic effects of fibrates (Ghonem *et al.*, 2015). In this study, NF-κB signalling in wild-type mice was inhibited in a dose-dependent manner and was unchanged in *Ppara*-null mice. These responses were in agreement with the reported role of PPARα in regulating NF-κB signalling. However, the effects of fenofibrate on cholestasis, which involve PPARα and are anti-inflammatory, were not mediated via inhibition of NF-κB. These observations do not support the classic view that NF-κB is involved in the inhibitory effects of fibrates on cholestatic liver injury (Ghonem *et al.*, 2015).

With regard to the STAT3 pathway, the p-STAT3 was slightly elevated in the WT-A group. In the wild-type groups pretreated with fenofibrate, the STAT3 pathway was inhibited in a dose-dependent manner. In *Ppara*-null mice, both the expression and phosphorylation of STAT3 were up-regulated in the KO-A and KO-A-F25 groups in which cholestasis and liver injury were evident. In agreement with these different effects on STAT3 signalling, the STAT3 target genes and the inflammatory factors were up-regulated more in *Ppara*-null mice than those in wild-type mice. The difference in STAT3 signalling between the two mouse lines was probably associated with upstream NF-κB signalling, which was inhibited by PPARα only in wild-type mice. More importantly, these differences indicated the different levels of effector molecules between the two mouse lines with cholestasis, even though their toxic phenotype was similar. Thus, these data suggest that NF-κB and STAT3 signalling contribute little to the protective action of fenofibrate.

JNK activation is usually mediated by inflammatory cytokines, including TNF-α, IL-1 and TGF-β (Weston and Davis, 2007). The synthesis and excretion of TNF-.alpha; and IL-1β is induced by bile acids in hepatic Kupffer cells (Miyake *et al.*, 2000). Cytokines, cholic acid and deoxycholic acid can in turn activate the JNK/c-Jun pathway (Li *et al.*, 2002; Higuchi *et al.*, 2004). In cellular models, the JNK pathway is associated with bile acid metabolism regulation (Gupta *et al.*, 2001; Li *et al.*, 2002; Li *et al.*, 2006). However, the JNK pathway has not been shown to have a critical role in *in vivo* cholestatic models. In this study, JNK signalling was activated in all the cholestatic groups of the two mouse lines, as indicated by increased levels of p-MKK4, p-JNK and c-Jun. This activation profile correlated well with cholestasis and liver injury, which was repeated in the WY14643 experiment. In the SP600125 experiment, the hepatic injury was substantially attenuated when JNK signalling was partially inhibited. Thus, the cholestatic associated liver injury was blocked by inhibition of the JNK pathway. Also SP600125 (WT-A-F-SP group) reversed the liver toxicity observed in the WT-A-F125 group. This result confirmed the involvement of JNK signalling in cholestatic liver injury and supports the conclusion in this study. Combining the above data in three individual experiments, the protection against the ANIT-induced intrahepatic cholestasis mediated by fenofibrate is thought to occur via inhibition of the JNK pathway. This protection is dependent on fenofibrate dose, as well as the presence of PPARα.

The protective effect of fenofibrate in cholestasis provides a basis for the prevention of cholestatic liver disease. The curative effects of fenofibrate in cholestasis were not investigated due to the strong self-healing of the positive model. Fibrate drugs are used clinically in combination with UDCA to treat cholestatic patients (Levy *et al.*, 2011). The effect of combination therapy with UDCA remains to be investigated. The ANIT-induced model of cholestasis was mainly used in this study, because it is a widely accepted cholestasis model

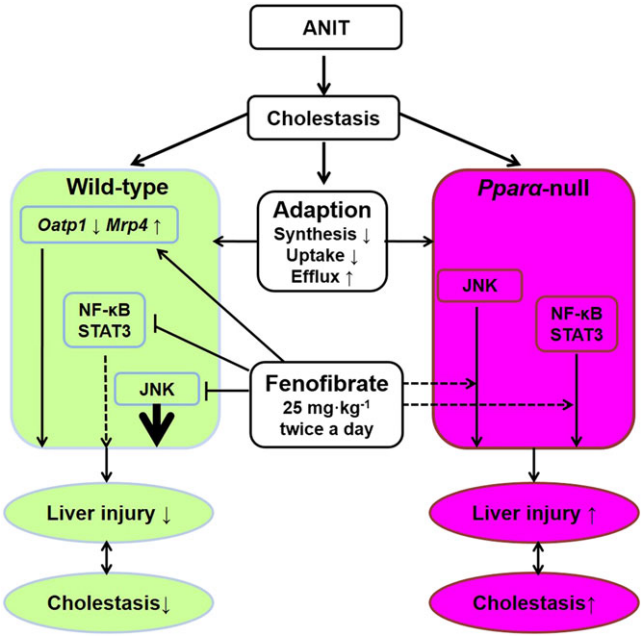


**Figure 10**

Proposed mode for the protection against intrahepatic cholestasis induced by fenofibrate. The protection involves inhibition of the JNK pathway and is dependent on both PPARα and the dose of the PPARα agonist. Solid lines denote biological responses, toxicological or pharmacological actions. Broken lines denote the responses or actions that contribute little to the indicated pathways or endpoints. Bold arrow of JNK pathway inhibition denotes that it is critically involved in the protective effects of fenofibrate.

and the pathological changes are very similar to those of human intrahepatic cholestatic liver disease (Goldfarb *et al.*, 1962; Fang *et al.*, 2016; Liu *et al.*, 2017). DDC was used as an animal model to study chronic PSC (Liedtke *et al.*, 2013). In this DDC model, fenofibrate also acted against cholestasis and liver injury, suggesting its effectiveness as a treatment for sclerosing cholangitis (Figure 9). However, it remains to be investigated whether this effect also involves JNK activation. Based on the above data, a model describing the findings in the present study is shown in Figure 10.

Taken together, the present results suggest that fenofibrate can effectively suppress cholestatic liver injury induced by ANIT and this protective effect occurred via inhibition of the JNK pathway. The dose–response relationship and dependence on PPARα of this effect of fenofibrate provide an important basis for clinical investigations of cholestasis treatment using fenofibrate. This widening of the pharmacological mechanisms of fenofibrate's protection against intrahepatic cholestasis offers further therapeutic opportunities for cholestatic liver diseases.

## Acknowledgements

This work was supported by National Natural Science Foundation of China (grants 81273582 and 81302848), Zhejiang Provincial Education Department (grant number Y201329949), Ningbo University Graduate Research Innovation Fund (G17116), the K.C. Wong Magna Fund in Ningbo University and the National Cancer Institute Intramural Research Program.

## Author contributions

M.D. and J.Y. performed most experiments, data collection, statistical analysis and data interpretation and wrote the manuscript; M.X., J.L and M.L. participated in the *in vivo* study; H.H., G.X., H.L. and D.S. analysed the data and revised the manuscript. Y.C. and B.G. performed LC–MS/MS analysis; J.Z. and F.J.G. revised the manuscript for important intellectual content; A.L. designed the overall study, supervised the experiments, analysed the results and wrote the paper.

## Conflict of interest

The authors declare no conflicts of interest.

## Declaration of transparency and scientific rigour

This Declaration acknowledges that this paper adheres to the principles for transparent reporting and scientific rigour of preclinical research recommended by funding agencies, publishers and other organisations engaged with supporting research.

## References

Alexander SPH, Cidlowski JA, Kelly E, Marrion N, Peters JA, Benson HE *et al.* (2015b). The Concise Guide to PHARMACOLOGY 2015/16: Nuclear hormone receptors. Br J Pharmacol 172: 5956–5978.

Alexander SPH, Fabbro D, Kelly E, Marrion N, Peters JA, Benson HE *et al.* (2015a). The Concise Guide to PHARMACOLOGY 2015/16: Enzymes. Br J Pharmacol 172: 6024–6109.

Alexander SPH, Kelly E, Marrion N, Peters JA, Benson HE, Faccenda E *et al.* (2015c). The Concise Guide to PHARMACOLOGY 2015/16: Transporters. Br J Pharmacol 172: 6110–6202.

Bergman AJ, Murphy G, Burke J, Zhao JJ, Valesky R, Liu L *et al.* (2004). Simvastatin does not have a clinically significant pharmacokinetic interaction with fenofibrate in humans. J Clin Pharmacol 44: 1054–1062.

Boonstra K, Beuers U, Ponsioen CY (2012). Epidemiology of primary sclerosing cholangitis and primary biliary cirrhosis: a systematic review. J Hepatol 56: 1181–1188.

Broome U, Olsson R, Loof L, Bodemar G, Hultcrantz R, Danielsson A *et al.* (1996). Natural history and prognostic factors in 305 Swedish patients with primary sclerosing cholangitis. Gut 38: 610–615.

Carbone M, Mells GF, Pells G, Dawwas MF, Newton JL, Heneghan MA *et al.* (2013). Sex and age are determinants of the clinical phenotype of primary biliary cirrhosis and response to ursodeoxycholic acid. Gastroenterology 144: 560–569.e567; quiz e513-564.

Cheung AC, Lapointe-Shaw L, Kowgier M, Meza-Cardona J, Hirschfield GM, Janssen HL *et al.* (2016). Combined ursodeoxycholic

acid (UDCA) and fenofibrate in primary biliary cholangitis patients with incomplete UDCA response may improve outcomes. Aliment Pharmacol Ther 43: 283–293.

Cindoruk M, Kerem M, Karakan T, Salman B, Akin O, Alper M *et al.* (2007). Peroxisome proliferators-activated alpha agonist treatment ameliorates hepatic damage in rats with obstructive jaundice: an experimental study. BMC Gastroenterol 7: 44.

Claessen MM, Vleggaar FP, Tytgat KM, Siersema PD, van Buuren HR (2009). High lifetime risk of cancer in primary sclerosing cholangitis. J Hepatol 50: 158–164.

Curtis MJ, Bond RA, Spina D, Ahluwalia A, Alexander SP, Giembycz MA *et al.* (2015). Experimental design and analysis and their reporting: new guidance for publication in BJP. Br J Pharmacol 172: 3461–3471.

Day AP, Feher MD, Chopra R, Mayne PD (1993). The effect of bezafibrate treatment on serum alkaline phosphatase isoenzyme activities. Metabolism: clinical and experimental 42: 839–842.

Delerive P, Gervois P, Fruchart JC, Staels B (2000). Induction of IkappaBalpha expression as a mechanism contributing to the anti-inflammatory activities of peroxisome proliferator-activated receptor-alpha activators. J Biol Chem 275: 36703–36707.

Dohmen K, Tanaka H, Haruno M (2013). Effectiveness of fenofibrate in comparison to bezafibrate for patients with asymptomatic primary biliary cirrhosis. Fukuoka igaku zasshi = Hukuoka acta medica 104: 350–361.

El-Sisi A, Hegazy S, El-Khateeb E (2013). Effects of three different fibrates on intrahepatic cholestasis experimentally induced in rats. PPAR Res 2013: 781348.

Fang ZZ, Tanaka N, Lu D, Jiang CT, Zhang WH, Zhang C *et al.* (2016). Role of the lipid-regulated NF-kappaB/IL-6/STAT3 axis in alpha-naphthyl isothiocyanate-induced liver injury. Arch Toxicol 91: 2235–2244.

Fievet C, Staels B (2009). Combination therapy of statins and fibrates in the management of cardiovascular risk. Curr Opin Lipidol 20: 505–511.

Ghonem NS, Ananthanarayanan M, Soroka CJ, Boyer JL (2014). Peroxisome proliferator-activated receptor alpha activates human multidrug resistance transporter 3/ATP-binding cassette protein subfamily B4 transcription and increases rat biliary phosphatidylcholine secretion. Hepatology 59: 1030–1042.

Ghonem NS, Assis DN, Boyer JL (2015). Fibrates and cholestasis. Hepatology 62: 635–643.

Goldfarb S, Singer EJ, Popper H (1962). Experimental cholangitis due to alpha-naphthyl-isothiocyanate (ANIT). Am J Pathol 40: 685–698.

Gupta S, Stravitz RT, Dent P, Hylemon PB (2001). Down-regulation of cholesterol 7alpha-hydroxylase (CYP7A1) gene expression by bile acids in primary rat hepatocytes is mediated by the c-Jun N-terminal kinase pathway. J Biol Chem 276: 15816–15822.

Harmer JA, Keech AC, Veillard AS, Skilton MR, Marwick TH, Watts GF *et al.* (2015). Fenofibrate effects on arterial endothelial function in adults with type 2 diabetes mellitus: a FIELD substudy. Atherosclerosis 242: 295–302.

Higuchi H, Grambihler A, Canbay A, Bronk SF, Gores GJ (2004). Bile acids up-regulate death receptor 5/TRAIL-receptor 2 expression via a c-Jun N-terminal kinase-dependent pathway involving Sp1. J Biol Chem 279: 51–60.

Hirschfield GM, Heathcote EJ, Gershwin ME (2010). Pathogenesis of cholestatic liver disease and therapeutic approaches. Gastroenterology 139: 1481–1496.

Hirschfield GM, Karlsen TH, Lindor KD, Adams DH (2013). Primary sclerosing cholangitis. Lancet 382: 1587–1599.

Honda A, Ikegami T, Nakamuta M, Miyazaki T, Iwamoto J, Hirayama T*et al.* (2013). Anticholestatic effects of bezafibrate in patients with primary biliary cirrhosis treated with ursodeoxycholic acid. Hepatology 57: 1931–1941.

Honda Y, Kessoku T, Ogawa Y, Tomeno W, Imajo K, Fujita K *et al.* (2017). Pemafibrate, a novel selective peroxisome proliferator-activated receptor alpha modulator, improves the pathogenesis in a rodent model of nonalcoholic steatohepatitis. Sci Rep 7: 42477.

Hunt MC, Yang YZ, Eggertsen G, Carneheim CM, Gafvels M, Einarsson C *et al.* (2000). The peroxisome proliferator-activated receptor alpha (PPARalpha) regulates bile acid biosynthesis. J Biol Chem 275: 28947–28953.

Kaplan MM, Poupon R (2009). Treatment with immunosuppressives in patients with primary biliary cirrhosis who fail to respond to ursodiol. Hepatology 50: 652.

Kilkenny C, Browne W, Cuthill IC, Emerson M, Altman DG (2010). Animal research: reporting *in vivo* experiments: the ARRIVE guidelines. Br J Pharmacol 160: 1577–1579.

Kok T, Bloks VW, Wolters H, Havinga R, Jansen PL, Staels B *et al.* (2003). Peroxisome proliferator-activated receptor alpha (PPARalpha)-mediated regulation of multidrug resistance 2 (Mdr2) expression and function in mice. Biochem J 369: 539–547.

Lazaridis KN, Talwalkar JA (2007). Clinical epidemiology of primary biliary cirrhosis: incidence, prevalence, and impact of therapy. J Clin Gastroenterol 41: 494–500.

Levy C, Peter JA, Nelson DR, Keach J, Petz J, Cabrera R *et al.* (2011). Pilot study: fenofibrate for patients with primary biliary cirrhosis and an incomplete response to ursodeoxycholic acid. Aliment Pharmacol Ther 33: 235–242.

Li D, Zimmerman TL, Thevananther S, Lee HY, Kurie JM, Karpen SJ (2002). Interleukin-1 beta-mediated suppression of RXR:RAR transactivation of the Ntcp promoter is JNK-dependent. J Biol Chem 277: 31416–31422.

Li F, Patterson AD, Krausz KW, Tanaka N, Gonzalez FJ (2012). Metabolomics reveals an essential role for peroxisome proliferator-activated receptor alpha in bile acid homeostasis. J Lipid Res 53: 1625–1635.

Li T, Jahan A, Chiang JY (2006). Bile acids and cytokines inhibit the human cholesterol 7 alpha-hydroxylase gene via the JNK/c-jun pathway in human liver cells. Hepatology 43: 1202–1210.

Liedtke C, Luedde T, Sauerbruch T, Scholten D, Streetz K, Tacke F *et al.* (2013). Experimental liver fibrosis research: update on animal models, legal issues and translational aspects. Fibrogenesis Tissue Repair 6: 19.

Lindkvist B, Benito de Valle M, Gullberg B, Bjornsson E (2010). Incidence and prevalence of primary sclerosing cholangitis in a defined adult population in Sweden. Hepatology 52: 571–577.

Liu A, Krausz KW, Fang ZZ, Brocker C, Qu A, Gonzalez FJ (2014a). Gemfibrozil disrupts lysophosphatidylcholine and bile acid homeostasis via PPARalpha and its relevance to hepatotoxicity. Arch Toxicol 88: 983–996.

Liu A, Tanaka N, Sun L, Guo B, Kim JH, Krausz KW*et al.* (2014b). Saikosaponin d protects against acetaminophen-induced hepatotoxicity by inhibiting NF-kappaB and STAT3 signaling. Chem Biol Interact 223C: 80–86.

Liu H, Liu Y, Wang L, Xu D, Lin B, Zhong R *et al.* (2010). Prevalence of primary biliary cirrhosis in adults referring hospital for annual health check-up in Southern China. BMC Gastroenterol 10: 100.

Liu Y, Liao X, Wang Y, Chen S, Sun Y, Lin Q *et al.* (2017). Autoantibody to MDM2: a potential serological marker of primary Sjogren's syndrome. Oncotarget 8: 14306–14313.

Martin PD, Dane AL, Schneck DW, Warwick MJ (2003). An open-label, randomized, three-way crossover trial of the effects of coadministration of rosuvastatin and fenofibrate on the pharmacokinetic properties of rosuvastatin and fenofibric acid in healthy male volunteers. Clin Ther 25: 459–471.

Marx N, Sukhova GK, Collins T, Libby P, Plutzky J (1999). PPARalpha activators inhibit cytokine-induced vascular cell adhesion molecule-1 expression in human endothelial cells. Circulation 99: 3125–3131.

Masana L, Cabre A, Heras M, Amigo N, Correig X, Martinez-Hervas S *et al.* (2015). Remarkable quantitative and qualitative differences in HDL after niacin or fenofibrate therapy in type 2 diabetic patients. Atherosclerosis 238: 213–219.

McGrath JC, Lilley E (2015). Implementing guidelines on reporting research using animals (ARRIVE etc.): new requirements for publication in BJP. Br J Pharmacol 172: 3189–3193.

Miyake JH, Wang SL, Davis RA (2000). Bile acid induction of cytokine expression by macrophages correlates with repression of hepatic cholesterol 7alpha-hydroxylase. J Biol Chem 275: 21805–21808.

Molodecky NA, Kareemi H, Parab R, Barkema HW, Quan H, Myers RP *et al.* (2011). Incidence of primary sclerosing cholangitis: a systematic review and meta-analysis. Hepatology 53: 1590–1599.

Nakamuta M, Enjoji M, Kotoh K, Shimohashi N, Tanabe Y (2005). Long-term fibrate treatment for PBC. J Gastroenterol 40: 546–547.

Patterson AD, Shah YM, Matsubara T, Krausz KW, Gonzalez FJ (2012). Peroxisome proliferator-activated receptor alpha induction of uncoupling protein 2 protects against acetaminophen-induced liver toxicity. Hepatology 56: 281–290.

Peters JM, Cheung C, Gonzalez FJ (2005). Peroxisome proliferator-activated receptor-alpha and liver cancer: where do we stand? J Mol Med 83: 774–785.

Pogson GW, Kindred LH, Carper BG (1999). Rhabdomyolysis and renal failure associated with cerivastatin-gemfibrozil combination therapy. Am J Cardiol 83: 1146.

Pollheimer MJ, Fickert P (2015). Animal models in primary biliary cirrhosis and primary sclerosing cholangitis. Clin Rev Allergy Immunol 48: 207–217.

Post SM, Duez H, Gervois PP, Staels B, Kuipers F, Princen HM (2001). Fibrates suppress bile acid synthesis via peroxisome proliferator–activated receptor-α–mediated downregulation of cholesterol 7α-hydroxylase and sterol 27-hydroxylase expression. Arterioscler Thromb Vasc Biol 21: 1840–1845.

Poupon R (2010). Primary biliary cirrhosis: a 2010 update. J Hepatol 52: 745–758.

Prince MI, James OF (2003). The epidemiology of primary biliary cirrhosis. Clin Liver Dis 7: 795–819.

Sakauchi F, Mori M, Zeniya M, Toda G (2005). A cross-sectional study of primary biliary cirrhosis in Japan: utilization of clinical data when patients applied to receive public financial aid. J Epidemiol 15: 24–28.

Sarma NJ, Tiriveedhi V, Crippin JS, Chapman WC, Mohanakumar T (2014). Hepatitis C virus-induced changes in microRNA 107 (miRNA-107) and miRNA-449a modulate CCL2 by targeting the interleukin-6 receptor complex in hepatitis. J Virol 88: 3733–3743.

Shirinsky I, Polovnikova O, Kalinovskaya N, Shirinsky V (2013). The effects of fenofibrate on inflammation and cardiovascular markers in patients with active rheumatoid arthritis: a pilot study. Rheumatol Int 33: 3045–3048.

Song D, Chu Z, Luo M, Tan Z, Li P, Han L *et al.* (2016). Gemfibrozil not fenofibrate decreases systemic glucose level via PPARα. Pharmazie 71: 205–212.

Southan C, Sharman JL, Benson HE, Faccenda E, Pawson AJ, Alexander SPH *et al.* (2016). The IUPHAR/BPS Guide to PHARMACOLOGY in 2016: towards curated quantitative interactions between 1300 protein targets and 6000 ligands. Nucleic Acids Res 44: D1054–D1068.

Tan Z, Liu A, Luo M, Yin X, Song D, Dai M *et al.* (2016). Geniposide inhibits alpha-naphthylisothiocyanate-induced intrahepatic cholestasis: the downregulation of STAT3 and NF [formula: see text]B signaling plays an important role. Am J Chin Med 44: 721–736.

Tischendorf JJ, Hecker H, Kruger M, Manns MP, Meier PN (2007). Characterization, outcome, and prognosis in 273 patients with primary sclerosing cholangitis: a single center study. Am J Gastroenterol 102: 107–114.

Walker LJ, Newton J, Jones DE, Bassendine MF (2009). Comment on biochemical response to ursodeoxycholic acid and long-term prognosis in primary biliary cirrhosis. Hepatology 49: 337–338 author reply 338.

Weston CR, Davis RJ (2007). The JNK signal transduction pathway. Curr Opin Cell Biol 19: 142–149.

Yang F, Xu Y, Xiong A, He Y, Yang L, Wan YJ *et al.* (2012). Evaluation of the protective effect of Rhei Radix et Rhizoma against alpha-naphthylisothiocyanate induced liver injury based on metabolic profile of bile acids. J Ethnopharmacol 144: 599–604.

Zhou X, Cao L, Jiang C, Xie Y, Cheng X, Krausz KW*et al.* (2014). PPARalpha-UGT axis activation represses intestinal FXR-FGF15 feedback signalling and exacerbates experimental colitis. Nat Commun 5: 4573.

## Supporting Information

Additional Supporting Information may be found online in the supporting information tab for this article.

https://doi.org/10.1111/bph.13928

**Table S1** A summary of dose-exposure relationship of fenfibric acid at steady state and dose extrapolation.
**Table S2** The primer sequences used in the Q-PCR analysis in this study.
**Figure S1** Determination of FA trough concentration at steady state. (A) The chromatograph and the supposed fragmentation pattern of FA. (B) The trough concentration of FA in serum at steady state. The mice were orally administered fenofibrate 5, 25, 125 $mg \cdot kg^{-1}$ twice a day for 5 day. Blood samples were collected 12 h after the last dose. The data were expressed as geometrical mean ± SD ($n$ = 5).
**Figure S2** Different regulated expression of genes involved in bile acid metabolism and transport in mouse liver. (A, B) *Bsep* mRNA level in two mouse lines. (C, D) *Ostb* mRNA level in wild-type and *Ppara*-null mice. The mRNA levels were measured by Q-PCR and normalized by 18S *rRNA*. mRNA levels in vehicle-treated control mice were set as 1 and results expressed as mean ± SD ($n$ = 5, *: compared with WT-C/KO-C; ^: compared with WT-A/KO-A; */^ $P < 0.05$).

**Figure S3** Differential transcription of the inflammatory genes associated with STAT3. (A, B) *Tnf-α* mRNA level in the wild-type and *Ppara*-null mice. (C, D) *Socs3* mRNA level in the wild-type and *Ppara*-null mice. (E, F) *Fga* mRNA level in the wild-type and *Ppara*-null mice. (G, H) *Fgb* mRNA level in the wild-type and *Ppara*-null mice. (I, J) *Fgg* mRNA level in the wild-type and *Ppara*-null mice. The mRNA levels were measured by Q-PCR and normalized by *18S rRNA*. mRNA levels in the vehicle-treated control mice were set as 1 and the results expressed as mean ± SD ($n$ = 5, *: compared with WT-C/KO-C; ^: compared with WT-A/KO-A; */^ $P < 0.05$).